British Journal of Pharmacology

British Journal of Pharmacology (2016) **173** 2880–2893 2880

RESEARCH PAPER

Effect of connexin 43 inhibition by the mimetic peptide Gap27 on corneal wound healing, inflammation and neovascularization

Correspondence Hossein Mostafa Elbadawy, Department of Pharmacology and Toxicology, College of Pharmacy, Taibah University, Universities Road, AlMadinah AlMunawwarah, Saudi Arabia. E-mail: hmbadawy@taibahu.edu.sa

Received 18 January 2016; **Revised** 30 June 2016; **Accepted** 16 July 2016

Hossein Mostafa Elbadawy[1,2], Pierfrancesco Mirabelli[3], Maria Xeroudaki[3], Mohit Parekh[2], Marina Bertolin[2], Claudia Breda[2], Carlo Cagini[4], Diego Ponzin[2], Neil Lagali[3]* and Stefano Ferrari[2]*

[1]Department of Pharmacology and Toxicology, College of Pharmacy, Taibah University, AlMadinah AlMunawwarah, Saudi Arabia, [2]International Center for Ocular Physiopathology, The Veneto Eye Bank Foundation, Venice, Italy, [3]Department of Ophthalmology, Institute for Clinical and Experimental Medicine, Faculty of Health Sciences, Linkoping University, Linkoping, Sweden, and [4]Department of Ophthalmology, Perugia General Hospital, University of Perugia, Perugia, Italy

*The two authors contributed equally to senior authorship.

BACKGROUND AND PURPOSE

The connexin 43 (Cx43) mimetic peptide Gap27 was designed to transiently block the function of this gap junction. This study was undertaken to investigate the effect of Gap27 on corneal healing, inflammation and neovascularization.

EXPERIMENTAL APPROACH

The effect of Gap27 on wound healing, inflammation and vascularization was assessed in primary human corneal epithelial cells (HCEC) *in vitro* and whole human corneas *ex vivo*, and in an *in vivo* rat wound healing model.

KEY RESULTS

Gap27 enhanced the wound closure of HCEC *in vitro* and accelerated wound closure and stratification of epithelium in human corneas *ex vivo*, but did not suppress the corneal release of inflammatory mediators IL-6 or TNF-α *in vivo*. In human corneas *ex vivo*, F4/80 positive macrophages were observed around the wound site. *In vivo*, topical Gap27 treatment enhanced the speed and density of early granulocyte infiltration into rat corneas. After 7 days, the expressions of TNF-α and TGFβ1 were elevated and correlated with inflammatory cell accumulation in the tissue. Additionally, Gap27 did not suppress VEGF release in organotypic culture, nor did it suppress early or late VEGFA expression or neovascularization *in vivo*.

CONCLUSIONS AND IMPLICATIONS

Gap27 can be effective in promoting the healing of superficial epithelial wounds, but in deep stromal wounds it has the potential to promote inflammatory cell migration and accumulation in the tissue and does not suppress the subsequent neovascularization response. These results support the proposal that Gap27 acts as a healing agent in the transient, early stages of corneal epithelial wounding.

Abbreviations

Cx43, connexin 43; K12, cytokeratin 12; GJA1, gap junction α 1; IHC, immunohistochemistry; ODN, oligodeoxynucleotides; HCEC, primary human corneal epithelial cells; SA, superfusion apparatus

DOI:10.1111/bph.13568

Tables of Links

TARGETS	
Other protein targets[a]	**Other ion channels**[b]
TNF-α	Cx43 (connexin 43)

LIGANDS	
IL-1β	TGFβ1
Il-6	VEGFA

These Tables list key protein targets and ligands in this article which are hyperlinked to corresponding entries in http://www.guidetopharmacology.org, the common portal for data from the IUPHAR/BPS Guide to PHARMACOLOGY (Southan *et al.*, 2016) and are permanently archived in the Concise Guide to PHARMACOLOGY 2015/16 ([a,b]Alexander *et al.*, 2015a,b).

Introduction

The success rate of ophthalmic procedures such as glaucoma filtration surgery, cataract extraction and corneal transplantation is greatly affected by post-operative wound healing in the cornea. Corneal wound healing is a multistep process where the stromal extracellular matrix proteins and growth factors excreted by the epithelium send the first signals of cell injury, followed by re-shaping of the epithelial cell. After initial closure of the wound, the limbus is activated to initiate the delivery of transient amplifying cells, which differentiate into basal epithelial cells. Basal epithelial cells start accumulating at the wound site and eventually migrate upwards to form a thicker, stratified corneal epithelium (Lu *et al.*, 2001; Castro-Munozledo, 2013).

Gap junctions form channels between adjacent cells. The gap junction α 1 (GJA1) gene encoding human connexin 43 (Cx43) was previously reported to be differentially expressed during wound healing (Coutinho *et al.*, 2003; Kretz *et al.*, 2003; Qiu *et al.*, 2003; Brandner, *et al.*, 2004; Söhl and Willecke, 2004). Alteration in the expression of Cx43 is associated with heart disease (Akar *et al.*, 2007) and cancer (McLachlan *et al.*, 2006; Li *et al.*, 2008). The basal layer of the corneal epithelium is known to exhibit Cx43 positivity, and the expression of Cx43 is down-regulated at the migrating edges of open wounds (Goliger and Paul, 1995; Matic *et al.*, 1997; Saitoh *et al.*, 1997; Coutinho *et al.*, 2003). A transient down-regulation of Cx43 is important in the initiation of the epithelial cell migration process in the early wound healing stages. This facilitates the uncoupling of adjacent connexons between cells, which is essential for epithelial cell migration to close the wound gap. This assertion has been validated by pharmacological and genetic targeting of Cx43, which can transiently block gap junctions' hemichannels to accelerate wound healing of vascular and avascular tissue. For example, antisense oligodeoxynucleotides (ODN) (Qiu *et al.*, 2003; Law *et al.*, 2006; Nakano *et al.*, 2008; Grupcheva *et al.*, 2012; Ormonde *et al.*, 2012) and siRNA (Nakano *et al.*, 2008) targeting Cx43 were successfully used to enhance the wound healing process in skin models. In rat models, ODN targeting Cx43 was also shown to promote corneal wound healing (Nakano *et al.*, 2008; Grupcheva *et al.*, 2012).

Gap27 is a synthetic peptide mimicking a sequence on the second external loop of the Cx43 hemichannel (Evans and Boitano, 2001). Treatment with the Cx43 mimetic peptide Gap27 has been reported to accelerate the healing in *ex vivo* skin models (Pollok *et al.*, 2011), human dermal fibroblasts *in vitro* (Wright *et al.*, 2012) and oral mucosal tissue *in vitro* (Tarzemany *et al.*, 2015); however, Gap27 has not yet been tested in the cornea, as a potential therapeutic agent for enhancing wound healing. In the present work, we evaluated the performance of Gap27 as a putative wound healing agent to accelerate the rate of wound healing in the cornea in the context of wounds of differing severity. The effect of Gap27 on corneal wound healing was tested on human corneal epithelium *in vitro* and in whole human corneas *ex vivo*. To investigate the effect of Gap27 on inflammation and angiogenesis, which are processes that cannot be accurately reproduced *in vitro*, a rat corneal *in vivo* model was used.

Methods

Human corneas for organotypic models

Human corneas were obtained with written consent from the donor's next of kin. The corneas with a previous history of injuries, stromal abnormalities, scars or major defects were excluded. The epithelial integrity and viability were checked using fluorescein dye (Sigma-Aldrich, Italy) and a Trypan blue (0.2%) exclusion assay (Sigma-Aldrich, Italy) respectively. Epithelium dehydration, oedema or defects were checked by light microscopy to confirm the presence of a healthy epithelium. Stromal opacity and the presence of scars or Descemet's folds were checked by slit lamp microscopy. Morphology of the endothelium, endothelial density, intracellular borders, polymorphism (pleomorphism and polymegathism), degeneration and dystrophy were evaluated by light microscopy. The inclusion criterion of endothelial cell density for this study was set at 1700–2200 cells·mm^{-2}, while for transplantation, corneas with at least 2200 cells·mm^{-2} are used.

Human corneal epithelial wound closure assays

The corneas were obtained from conventional organ culture conditions within 1 week *post-mortem*. Epithelial cells from limbal biopsies were used in *in vitro* wound healing assays. Co-culture of limbal stem cells with 3T3 cells was performed as previously reported (Di Iorio *et al.*, 2010). Biopsies of 1 mm^3 from the limbal region of five human donor corneas were minced and trypsinized (0.05% trypsin/0.01% EDTA; Life Technologies, Italy) at 37°C for 3–4 cycles of 30 min each. Once isolated, cells were plated (4.8×10^4 cm^{-2}) onto lethally irradiated 3T3-J2 cells (2.4×10^4 cm^{-2}) and cultured in 5% CO_2, using a mixture of DMEM (Life Technologies, Italy) and Ham's F12 (Life Technologies, Italy) media (2:1) containing FCS (10%; Life Technologies, Italy), penicillin-

streptomycin (50 U·mL^{-1} 1%; Euroclone, Italy), glutamine (4 nM 2%; Euroclone, Italy), insulin (Humulin 5 μg·mL^{-1}; Eli Lilly Canada), adenine (0.18 mM; Merck Millipore, Italy), hydrocortisone (0.4 μg·mL^{-2}; Merck Millipore, Italy), cholera toxin (8.1 μg; Sigma-Aldrich, Italy), triiodothyronine (2 nM; Sigma-Aldrich, Italy) and EGF (10 ng·mL^{-1}; Austral Biological, USA). Sub-confluent primary cultures were trypsinized, plated at a density of 1.1 × 10^4 cells·cm^{-2} and cultured in tissue culture inserts (Ibidi, Germany) in an organ culture incubator (31°C, 5% CO_2). The inserts has two chambers in which primary human corneal epithelial cells (HCEC), and 3T3-J2 fibroblasts were co-cultured, with a 0.5 mm barrier between the chambers. When the insert is removed, two islets of cells are formed and the cells migrate to close a gap. When cells reached confluence, 10 cultures were treated (for 1 h prior to the removal of the insert) with either Gap27 or scGap27 (Gap27 is the test agent, and the control peptide, scGap27, is the scrambled version of Gap27) in serum-free medium (five cultures each) at a final concentration of 0.1 mM (Pollok *et al.*, 2011). Gap27 was reported to lose its effect after 12 h in culture (Wright *et al.*, 2009). The insert was then removed, and cells were allowed to migrate to close the gap. Treatment was then repeated every 24 h after removal of the insert. From each biopsy, one culture served as a control treated with scGap27 (n = 5) and the second was treated with Gap27 (n = 5). Images were taken at fixed time points, and the width of the gap was measured from microscopic images using ZEN software (Carl Zeiss, Germany). Investigators were blinded to the treatment by masking the labelling of the eye drops, and blinding was continued throughout the experimental and image analysis phase.

Human corneal wound healing ex vivo model

The human corneal superfusion apparatus (SA) is an artificial human corneal environment designed and developed in our lab to mimic the human cornea in its natural environment (Elbadawy *et al.*, 2015). Organ culture corneas used for these experiments were maintained at 31°C in storage media. Storage media consisted of a base of Eagle's MEM supplemented with penicillin, streptomycin, fungicide (amphotericin B or nystatin) and 10% FCS. A storage period of 30 days can be achieved without significant loss of endothelial cells. The experiments were performed under sterile conditions and controlled temperature (31°C) with regular flow of artificial tears (PBS with 10% FBS; two drops of 30 μL·min^{-1}). Ten pairs of corneas were used for wound healing *ex vivo* experiments using a fluorescein penetration test to follow the healing of the epithelium (n = 10). The corneas were equilibrated in the SA for 1 day prior to experimentation. On the following day, a wound was induced across the corneal surface using an AlgerBrush II (Alger Company, Inc, Lago Vista, TX, USA) equipped with a rotating 0.5 mm burr to reproduce a regular wound by brushing away approximately 500 μm of corneal tissue epithelium without penetrating the Bowman layer. The corneas were incubated with either Gap27 or scGap27 (1 mM) in serum-free medium, maintained in organ culture for 1 h after injury, and the treatment was repeated once daily. The corneas were returned to the SA with constant tear flow and were allowed to heal for up to 7 days. Time points selected were pretreatment, post injury, 6 h, 1, 3, 5 and 7 days. At each time point, the fluorescein penetration test was performed to follow the wound closure progress, and trypan blue was used prior to measuring the wound width using microscopic images analysed by ZEN software.

To examine corneal wound healing in different layers of the cornea, 42 corneas incubated in organ culture for 2 to 3 weeks *post-mortem* were divided into two equal groups. The first group was treated with Gap27 and the second with scGap27, and the wound healing assay was performed using the SA as above. At each time point, six corneas were fixed in 4% PFA, sectioned (sections of 10 μm) and were used for immunohistochemistry (IHC) and apoptosis assays.

For quantification of the release of proteins, including TNF-α, IL-6 and VEGF after inducing a wound to the ocular surface of human corneas using the AlgerBrushII as detailed above, a submerged culture model of human corneas was used as described in the protein detection using ELISA section. Investigators were blinded to the treatment by masking the labelling of the eye drops, and blinding was continued throughout the experimental and image analysis phase by the use of randomly assigned numeric identifiers.

Rat corneal stromal wounding in vivo model

Animal studies are reported in compliance with the ARRIVE guidelines (Kilkenny *et al.*, 2010; McGrath and Lilley, 2015).

Animal experiments were reviewed by the Linköping Regional Animal Ethical Committee, and permission to conduct the experiments was granted (Protocol No. 7–13). The care and use of animals followed the guidelines set out in the EU Directive 2010/63/EU on the protection of animals used for scientific purposes and adhered to the principles of the Association for Research in Vision and Ophthalmology Guidelines for the Use of Animals in Ophthalmic and Vision Research. A model of corneal injury in Wistar rat was chosen because preclinical studies of ocular therapeutics are often conducted in rodents, which have similar pathological characteristics to human (Peebo *et al.*, 2011). Rat cornea is large enough to enable *in vivo* imaging of inflammation while still being a small animal model. Animals were maintained in a licensed care facility in a room with ventilation (15 air changes h^{-1}), temperature 22 ± 2°C, humidity 55 ± 10%, 12 h light/dark cycle, with a background sound of max 55 dB. The rats were housed per rectangular cage, with cage volume of 1760 cm^2. Cages were outfitted with wood chips, shredded paper products, tunnels to hide in and wooden pegs. Access to food and water was *ad libitum*. Humane endpoints were used according to an institutional scoring system. Specifically, if the general health condition, movements, breathing, skin and hair were noticeably affected, then a score was given, and if a minimum score was exceeded, the animal was humanely killed.

The model consisted in a surgical suture-induced corneal inflammation and neovascularization in rats, as described previously (Mirabelli *et al.*, 2014). 32 male Wistar rats 12–16 weeks old and weighting 300–400 g (Scanbur AB, Sollentuna, Sweden) were used. For general anaesthesia, each animal received the anaesthetic Ketanest (esketamine 25-mg·mL^{-1}, 0.4 mL; Pfizer, Sollentuna, Sweden) and analgesic Dexdomitor (dexmedetomidine hydrochloride 0.5 mg·mL^{-1}, 0.2 mL; Orion Pharma, Espoo, Finland) by i.p. injection. Additionally, one drop of topical anaesthesia was also applied to the eye prior to surgical and ophthalmic imaging

procedures (tetracaine hydrochloride 1%; Chauvin Pharmaceuticals, London, UK). Under local and systemic anaesthesia, a corneal stromal suture was placed 1.5 mm from the temporal limbus in one eye per animal. Immediately following surgical suture placement, antibiotic eye ointment was applied (Fucithalmic, fucidic acid 1%; Abcur, Helsingborg, Sweden) as an antiseptic and lubricant. After suturing, rats were randomly assigned to two groups and treated with experimental eye drops prepared from ice-cold peptide dissolved in PBS (calcium-free and magnesium-free). The first group (16 rats) was treated with scGap27 and the second group (16 rats) with Gap27. Eye drops were instilled in the sutured eye four times daily at a concentration of 1 mM. Animals were euthanized while under general anaesthesia by intracardial injection of 1 mL of sodium pentobarbital 60-mg·mL^{-1}(APL, Stockholm, Sweden). Following an experimental session, anaesthesia was reversed by s.c. injection of , 0.1 mL of antisedan (atipamezole 5 mg mL^{-1}; Orion Pharma, Espoo, Finland). All animals recovered consciousness after surgery, and no postoperative analgesia was applied as the procedure is considered very mild and the general behaviour of the animals did not indicate ocular pain or discomfort. The first application of experimental or sham substances was given while animals were under general anaesthesia, whereas all subsequent applications were given while animals were fully awake.

Half of the rats of each group were killed after 2 days and the second group after 7 days. At 2 or 7 days, corneas were collected and frozen at −80°C for histology (one cornea per group per time point) or −20°C for RNA extraction for RT-PCR (seven corneas per group per time point). *In vivo* confocal microscopy was performed longitudinally in rat corneas as described previously (Mirabelli *et al.*, 2014). Rats were randomized to different experimental groups after surgery by assigning a study number to each rat. Analysis of experimental data (photographs, *in vivo* confocal images) was performed in a masked manner with only study numbers visible and without knowledge of group membership. After completion of measurements, group data were compiled for statistical comparisons.

Investigators were blinded to the treatment by masked labelling of the eye drops, and blinding was continued throughout the experimental and image analysis phase by the use of randomly assigned numerical identifiers for each rat and labelling as Group 1 and 2 to mask the treatment.

Immunohistochemistry

Corneal sections from the 7 days *ex vivo* wound healing assay were brought to room temperature (RT), washed twice with PBS, permeabilized with 0.5% Triton X-100 (Sigma-Aldrich, Life Technologies, Milan, Italy) at RT for 30 min then washed three times with PBS. Two hours coating was performed in blocking buffer composed of 0.2% BSA (Sigma-Aldrich, Life Technologies, Milan, Italy), 2% goat serum (Sigma-Aldrich, Life Technologies, Milan, Italy) and 0.2% Triton X-100 in PBS at RT. Primary antibodies (1:100 unless in the blocking mix) were added and incubated overnight at 4 °C then for 2 h at RT. Primary antibodies used were F4/80 (Abcam, UK), myeloperoxidase (MPO; Abcam, UK), Cx43; Cell signalling biotechnologies, Italy) and actin (Santa Cruz, Italy). All primary antibodies were used at a concentration of 1:100. Three washing steps (5 min each) with PBS were carried out. Anti-mouse, rat or rabbit (1:1000) conjugated with FITC secondary antibodies (Santa Cruz, Terracina, Italy) diluted in 0.2% BSA/PBS were added for 2 h at RT. Three washing steps (5 min for each) with PBS were then carried out. Sections were then mounted in DAPI-containing media and an LSM-510 meta confocal laser microscope (Carl Zeiss, Oberkochen, Germany) was used to detect fluorescence.

Protein detection using ELISA

Six corneas from three donors were used so that for each pair, one eye was treated with scGap27 and the other with Gap27. The corneas were obtained from conventional organ culture conditions after storage for 1 to 2 weeks *post-mortem*. The corneas were maintained submerged in 3 mL of storage media, and quantification of VEGF, TNF-α and IL-6 released in the media was performed using ELISA kits for human TNF-α and IL-6 (Sigma-Aldrich, Italy), and for VEGF (Life Technologies, Milan, Italy), by following the manufacturers' protocols. A wound was induced across the corneal surface using an AlgerBrush II, and corneas were treated for 1 h with either 1 mM of scGap27 or Gap27 in serum-free medium. For each time point, the media was changed 1 h before collection; therefore, the amount of protein detected in each collected sample corresponded to the release of this protein during the 1 h before the collection time point. Media collected for ELISA were given numbers in the same manner as described above, and ELISAs were performed blindly by three investigators, and results were analysed independently then combined for statistical analysis.

Real time quantitative PCR on rat corneal extracts

Total RNA from each corneal sample was isolated with Qiagen RNeasy Mini Kit (Qiagen, Hilden, Germany). RNA concentrations were determined using a Nanodrop ND-2000 spectrophotometer (Nano Drop Technologies Inc, Wilmington, Delaware, USA), and the cDNA was synthesized from the total RNA (100 ng) using a SuperScript® VILO™ cDNA Synthesis Kit (Invitrogen, UK) in accordance with the manufacturer's instructions. PCR reactions were performed on all corneal samples using TaqMan Fast Advanced Master Mix and TaqMan Gene Expression Assays (Applied Biosystems, Carlsbad, California, USA) in a total volume of 20 mL. Real-time PCR conditions were 50°C for 2 min, 95°C for 1 min and then 40 cycles of 95°C for 15 s, 60°C for 20s. The primers (Applied Biosystems, Carlsbad, California, USA) used for PCR analysis were as follows: rat IL-6, VEGFA, TNF-α, IL-1β, TGFβ and GJA1. The mRNA expression level for each gene was calculated by the ΔCt method using GAPDH as a housekeeping control gene. Real-time PCR was run in triplicate for each corneal sample, and gene expression of triplicates was averaged, referenced to GAPDH, and reported relative to the average relative expression level in three negative control samples (corneas from non-sutured rats). All reactions were carried out using an ABI PRISM 7900HT Real-Time PCR system (Applied Biosystems, Carlsbad, California, USA). RT-PCR data are expressed as fold change normalized to naïve corneas to indicate the level of gene expression relative to healthy, non-operated tissue.

Biodistribution of Gap27 in human corneas

To study the penetration of Gap27 in the corneal layers, a custom Gap27 was synthesized containing a fluorescent probe (FITC). The sequence of the protein was FITC-SRPTEKTIFII designed and synthesized by ProteoGenix (France). Five couples of corneas were used. Left eye corneas were treated with the regular Gap27 and corresponding right eye corneas were treated with the labelled Gap27 peptide (Gap27-FITC). The corneas were rinsed thoroughly and then incubated in organ culture media for 2 h then fixed in 4% PFA. Sections were cut as described before and stained with DAPI and dye stabilizer. Dye-only controls were performed using FITC dye added after fixing in PFA. Positivity was checked using an LSM-510 meta confocal laser scanning microscope (Carl Zeiss, Germany) to detect fluorescence.

Histology of rat corneal tissue

The corneas were fixed in 4% paraformaldehyde (PFA; Santa Cruz, DBA, Italy) overnight and washed in 7.5, 15 then 30% sucrose solution sequentially for 30 min each. The corneas were then incorporated in optimal cutting temperature compound, flash frozen and stored at −80°C. Sections (10 μm) were obtained for histological and immunofluorescence. Haematoxylin and eosin staining was performed for standard histology. Fixed samples (4% PFA) were rehydrated in distilled water, exposed to Harris haematoxylin (Sigma Aldrich, Milan, Italy) for 8 min and then washed three times with tap water for 5 min each. Differentiation solution (Sigma-Aldrich, Italy) was added then the samples were briefly washed with tap water. Samples were further exposed to Eosin (Sigma-Aldrich, Italy) for 2 min then washed with tap water as before. Sections were washed in an increasing concentration of alcohol (70, 90 and 100%) followed by xylol (Sigma-Aldrich, Italy) treatment for 3 min each. Xylene-based mounting medium (Sigma-Aldrich, Italy) was used to mount and preserve the samples, which were examined using light microscopy. ZEN software was used to capture the images.

TUNEL assay of human corneas ex vivo model

Cell apoptosis was assessed using a TUNEL assay. The manufacturer's protocol was followed for the TACS 2 terminal deoxynucleotidyl transferase diaminobenzidine (DAB) *in situ* apoptosis detection kit (Trevigen, USA). Three samples treated with scGap27 or Gap27 were analysed for each time point (pretreatment, 6 h, 1, 3, 5 and 7 days). Images were analysed using the ZEN software.

Data analysis

Prior to statistical analysis of *in vivo* data, treatment and group identity were unmasked. To compare inflammatory cell density and migration distance between Gap27 and scGap27 groups *in vivo*, the Mann–Whitney rank sum test was used. Gene expression differences, vascularized area, inflammatory cell density, cell migration and distance and limbal vessel diameter were independently assessed by three observers following a previously published protocol (Mirabelli *et al.*, 2014), and the average values across observers were used for analysis.

For all *in vitro* results, data from three blinded investigators were used for independent *t*-test. Statistical analyses were performed using SigmaStat 3.1 software for Windows (Systat Software Inc., Chicago, USA) and GraphPad InStat (GraphPad Software, Inc. USA). Tests were two-tailed, and the level of probability (P) deemed to constitute the threshold of statistical significance was set at $P < 0.05$ for all experiments. The data and statistical analysis comply with the recommendations on experimental design and analysis in pharmacology (Curtis *et al.*, 2015).

Materials

The pharmacological agent Gap27 peptide (SRPTEKTIFII) was purchased from Tocris (UK) and Eurogentec (Belgium), and its scrambled (sham) version scGap27 (REKIITSFIPT) was purchased from Eurogentec (Belgium). Gap27-tagged peptides were custom-made by ProteoGenix (France). Peptides were dissolved in calcium- and magnesium-free sterile saline solution, and treatment was carried out using 1 mM of either Gap27 or scGap27 for *in vivo* and *ex vivo* experiments and 0.1 mM for *in vitro* experiments.

Results

Gap27 accelerates wound closure in vitro

Treatment with Gap27 primed HCEC to initiate the closure of the 0.5 mm gap faster than cultures treated with scGap27 (Figure 1, $P < 0.001$). The rate of gap closure varied between cells obtained from biopsies of different donors. However, the healing process started 6 h post injury and progressed to close the gap completely after 24–27 h in five cultures treated with Gap27 (Figure 1B). In cultures treated with scGap27, the commencement of gap closure was delayed by 24 h. Complete gap closure was seen within 9 h thereafter in three cultures and after a total of 48 h in two cultures (Figure 1A).

Wound healing of human corneas ex vivo is accelerated by Gap27

An organotypic wound healing assay using human corneas maintained in an artificial environment, the SA, was performed over 7 days. Pairs of corneas from 10 donors were used so that for each pair, one eye was treated with scGap27 and the other with Gap27. Wound closure occurred after 3 days, when no fluorescein uptake was noticed. Afterwards, until day 7 of these experiments, all corneas were negative for fluorescein dye uptake (Figure 2A). Transverse sections were taken from each time point and stained with anti-actin antibody using IHC (Figure 2B). The epithelialization profile showed that after 6 h, wound edges were clearly seen under both conditions. However, after 1 day, a monolayer of migrating cells closed the wound in Gap27-treated corneas ($P < 0.05$) but not in the scGap27 group (Figure 2C). On day 3, Gap27-treated corneas had regenerated a multi-layered epithelium with uniform thickness and actin distribution, whereas scGap27-treated corneas exhibited irregular epithelial thickness and actin distribution. By day 5, a full epithelium had regenerated under both conditions, but the Gap27-treated corneas had a more uniformly stratified epithelium with a well-defined basal epithelial layer. By day 7, the wounded area appeared identical to the unwounded epithelial layer under both treatments. In the Gap27 group, the wound completely

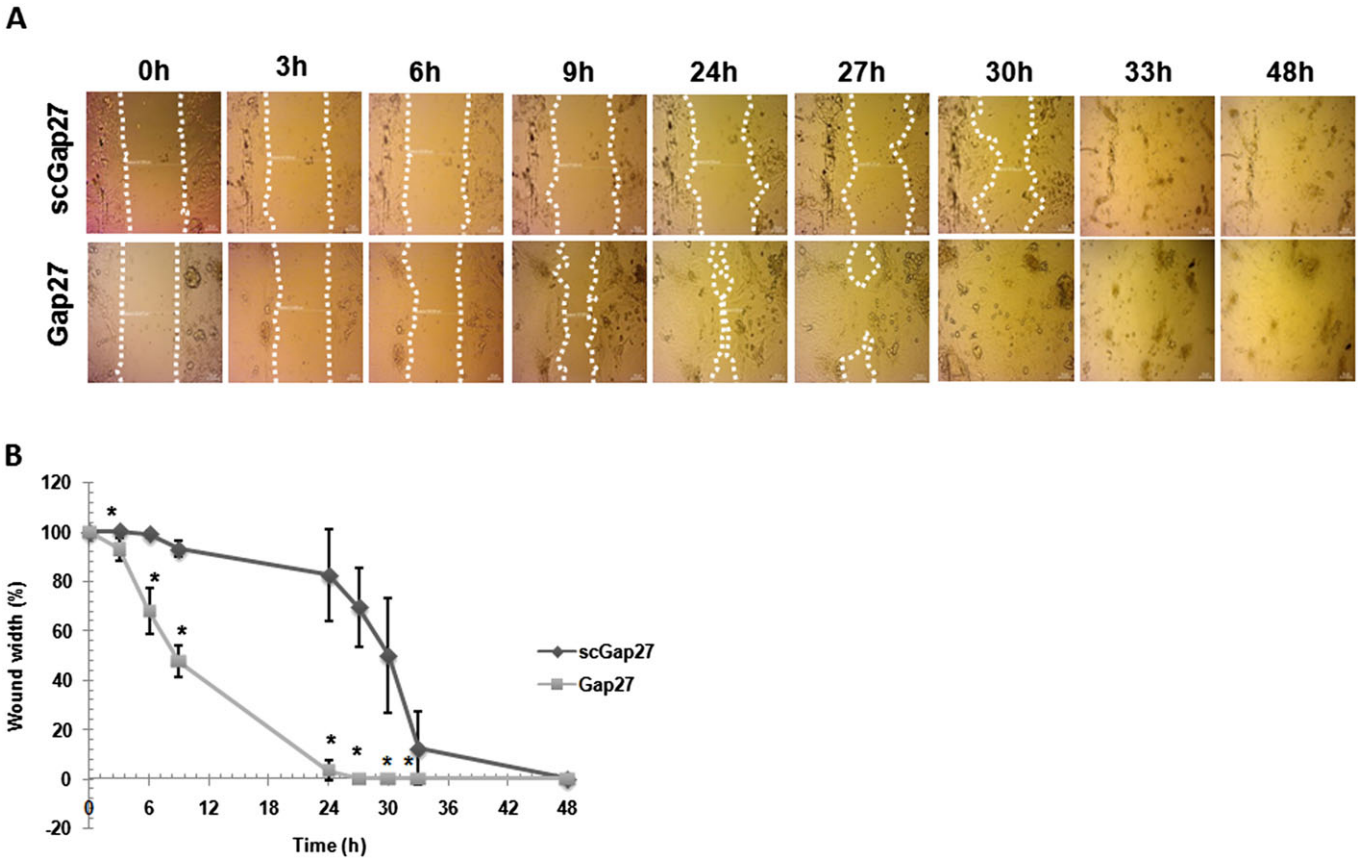

Figure 1

Gap27 promotes corneal epithelial wound closure *in vitro.* Each image is representative of five images ($n = 5$) taken using a light microscope (20X). The migrating edges were outlined using the white dotted line (A). The gap width was calculated as a percentage of that at 0 h (100%) until total closure of the gap (0%). Epithelialization rate of cultures treated with scGap27 is significantly lower than those treated with Gap27 (B). * Indicates significant differences in Gap27-treated cultures compared with scGap27 where $P < 0.05$.

closed on day 1 in eight corneas and on day 3, in two corneas; in the scGap27 group, the wound closed after 3 days in all corneas (Figures 2A and B). Gap27-FITC showed positivity near the wound edges and in the adjacent peripheral area, in the basal layer of the epithelium (Figure 2D). Additionally, stromal positivity was detected in close proximity to the nuclei of the stromal keratocytes, which were counterstained with DAPI nuclear staining indicating good penetration of Gap27-FITC through the damaged epithelium and into the stroma of human corneas (Figure 2D). However, fluorescence was not seen in the stroma underneath intact epithelium. No fluorescence was observed in any of the corneas treated with non-fluorescent Gap27.

The expression pattern of Cx43 during the healing of corneal epithelium in Gap27-treated corneas was not different from corneas treated with scGap27 for 7 days (Supporting Information Figure S1). Cx43 expression was concentrated in the basal layer of the epithelium and stroma, while at the wound edges, Cx43 was also detected in the upper epithelial layers. Gap27 treatment did not change the expression pattern of Cx43, nor did it alter the expression of zonula occludens-1, a major component of the tight junction, which was expressed at all times. This indicated that Gap27 had no effect on the epithelial barrier function (Supporting Information Figure S1). The expression of the epithelialization marker cytokeratin 12 (K12) and the limbal stem cell marker p63 was performed on all sections to ensure general quality of the corneas throughout the experiment and normal wound healing response of the corneas. The expression of the epithelialization marker K12 was detectable in the epithelium of all corneas, while the limbal stem cells marker p63 was expressed in the limbus area as well as in the basal layer of the epithelium. There were no significant differences between groups treated with scGap27 or Gap27 throughout the experimental period (Supporting Information Figure S1). To study the effect of Gap27 on the viability of the layers of the cornea, corneal sections from each time point were used for the TUNEL assay. Treatment with Gap27 or scGap27 did not appear to cause cell apoptosis in any layer of the corneas at any time (Supporting Information Figure S2). Additionally, the uninvolved areas of the epithelium were negative for Trypan blue staining at all stages.

Gap27 and corneal inflammation

The *ex vivo* submerged culture model was used to study corneal release of inflammation mediators in the media using

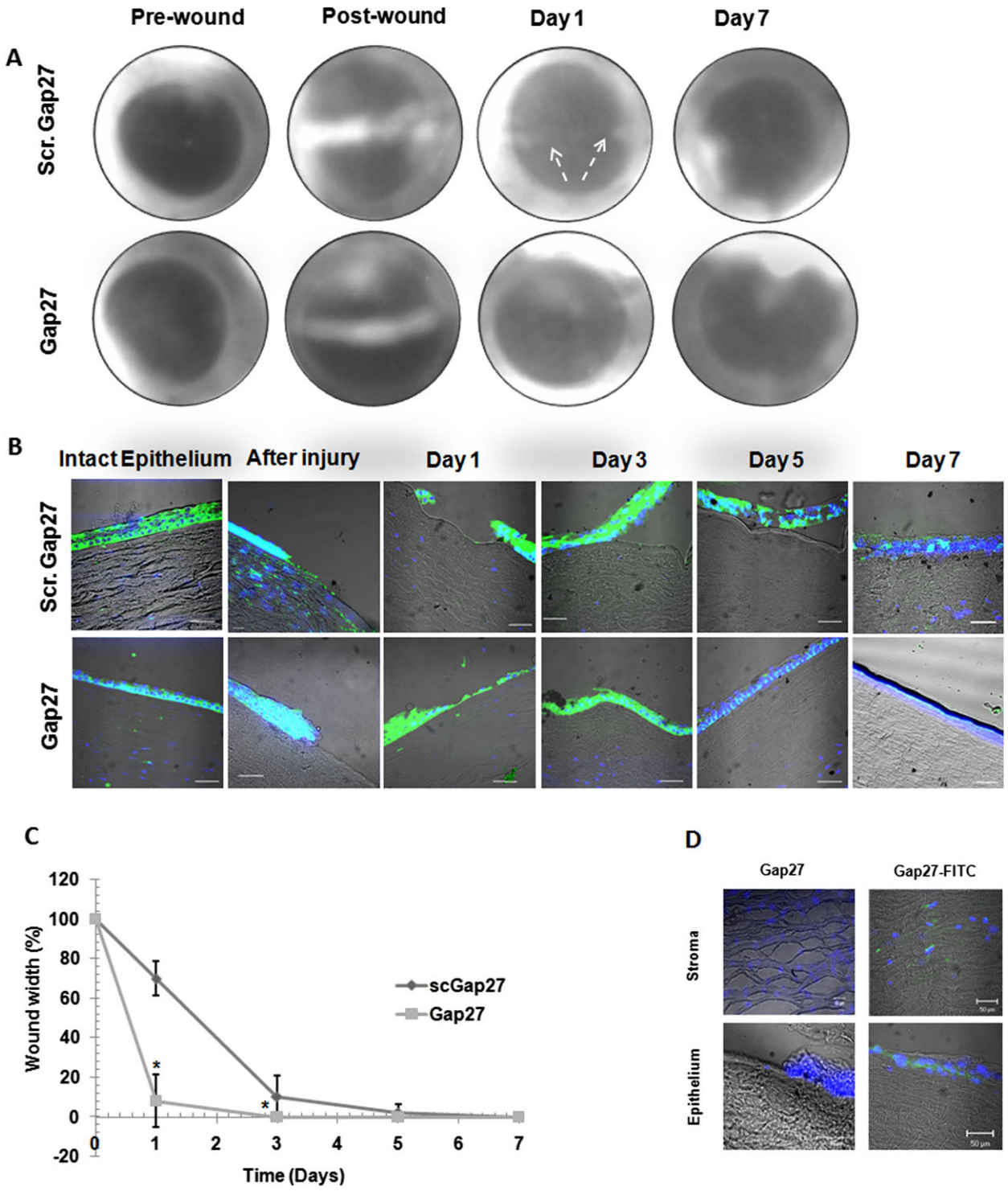

Figure 2

Gap27 accelerates epithelial wound closure and stratification of the corneal epithelium in an *ex vivo* model. In a human corneal *ex vivo* model, progression of corneal wound closure was observed using fluorescein ophthalmic dye. Each image is representative of 10 images for pairs of corneas treated with either scGap27 or Gap27 (A). Transverse sections stained with FITC-conjugated antibody attached to anti-actin primary antibody (green) showed the re-epithelialization of corneas treated with scGap27 (top row) or Gap27 (bottom row). Nuclei were labelled with DAPI (blue). Images were taken using the 40× lens and scale bars are 10 μm (B). Each image is representative of three corneas per time point ($n = 3$). Wound closure rate during 7 days was calculated ($n = 10$) as a percentage of that at 0 h (100%) until total closure of the gap (0%) and is shown in (C). In (D), Gap27 peptide labelled with a fluorescent probe (FITC) was detectable in the stroma (top row) and epithelium (bottom row) of corneas ($n = 5$) treated with Gap27-FITC (green). Nuclei were labelled with DAPI (blue). Images were taken using 40× lens of the laser scanning confocal microscope. * Indicates significant differences in Gap27-treated cultures compared with scGap27 where $P < 0.05$.

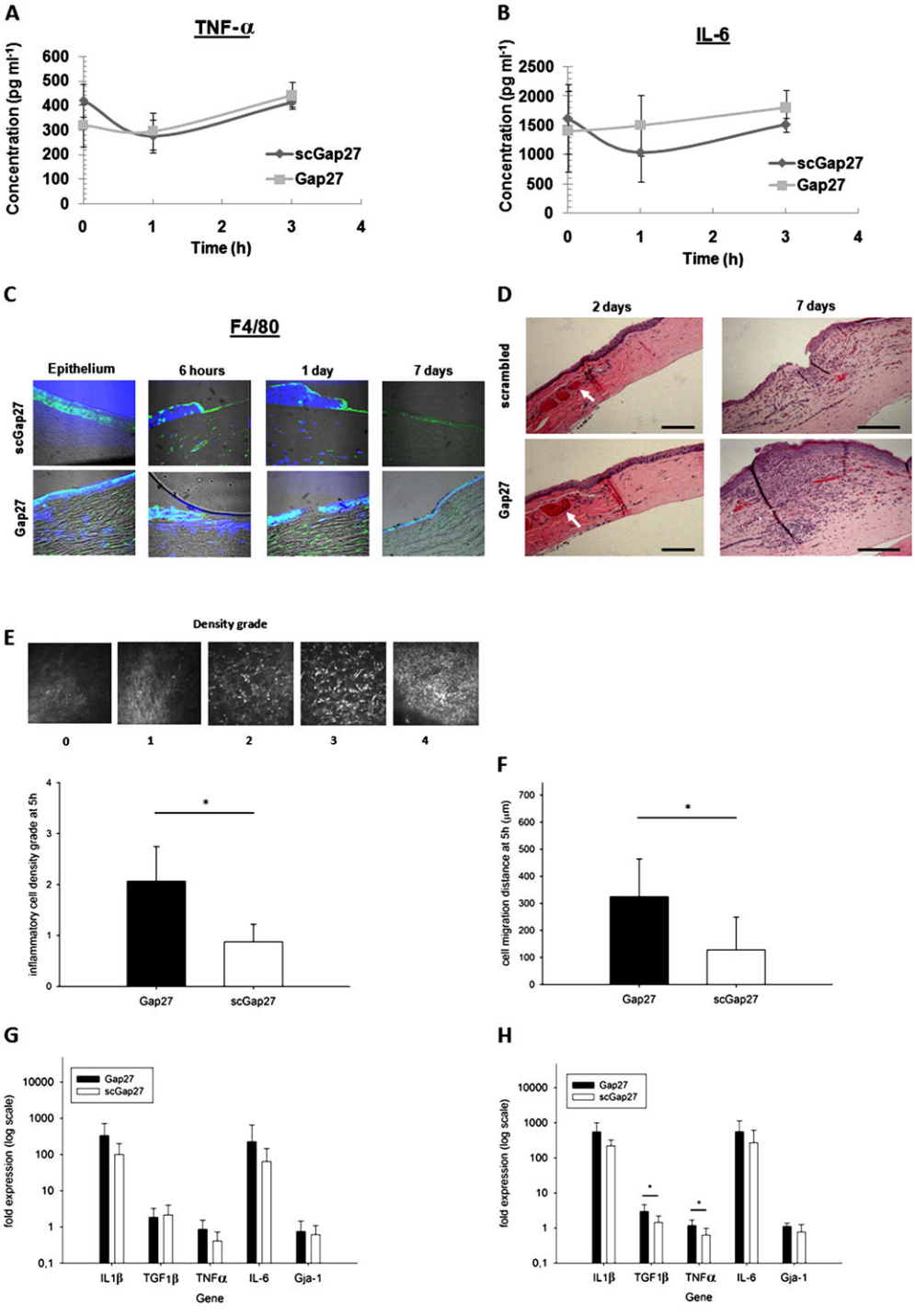

Figure 3

Gap27 enhances inflammatory cell migration and accumulation in response to injury in the organotypic culture and *in vivo* corneal inflammation models. The release of TNF-α (A) and IL-6 (B) during the early wound healing stage of human corneas ($n = 3$) *ex vivo* treated with either scGap27 or Gap27. The expression of the marker of activated macrophages F4/80 (C) detected using specific antibody labelled with FITC-conjugated secondary antibody (green). Nuclei were labelled with DAPI (blue). Images are representative of three images from three corneas taken using 40× lens of the laser scanning confocal microscope. Using the *in vivo* rat model, a representative cornea from each treatment group was used, showing distinct changes in corneas stained with haematoxylin and eosin (D). Images were taken using the 10× lens of a light microscope fitted with a digital camera. Scale bars are 100 μm, and arrows indicate dilated limbal vessels. Quantification of inflammatory cell densities (E) and their migration distances (F) from the limbus using *in vivo* confocal microscopy are shown. A grading system was used to evaluate inflammatory cells' densities as shown in (E; top panel). Images are 400 × 400 μm. Gene expression of IL-1β, TGFβ1, TNF-α, IL-6 and Gja-1 was quantified using RT-PCR after 2 (G) and 7 days (H) using corneas from the rat *in vivo* model ($n = 7$). Error bars represent SD. * Indicates significant differences in Gap27-treated cultures compared with scGap27 where $P < 0.05$.

ELISA. The release of TNF-α was decreased after 1 h in both scGap27- and Gap27-treated corneas. This decrease was reversed after 3 h in both cases (Figure 3A). The release of IL-6 from corneas at 1 h after treatment was reduced compared with pretreatment levels in scGap27-treated corneas but not in Gap27-treated corneas, where IL-6 levels were maintained (Figure 3B). No absolute changes in TNF-α or IL-6 expression were noted between scGap27 and Gap27 treatment groups (Figure 3A and 3B).

To detect the expression of inflammatory cell markers during a prolonged wound healing assay (7 days), transverse corneal sections were taken at all time points from the *ex vivo* wound healing experiment using our culture system (the SA). Sections from three corneas per treatment per time point were stained against the marker of activated macrophage F4/80. Macrophage marker F4/80 was detectable in the epithelium and the stroma and was more abundant in the stroma underneath uninvolved epithelium in Gap27-treated corneas. The expression of F4/80 was detected in the stroma underneath the wound site and in the epithelium of scGap27-treated corneas to a lesser extent, compared with the Gap27 group. After 1 day, Gap27-treated corneas exhibited strong F4/80 staining, which was barely detectable at 3-days, when F4/80 was abundant in the epithelium of scGap27-treated corneas. By 7 days, the corneas recovered with minor fluorescence detected in the stroma below the wound site in both scGap27- and Gap27-treated groups (Figure 3C).

In the *in vivo* rat model, placing a suture in rat corneas induced a mild thickening of the epithelium in the Gap27 group at 2 days and substantial stromal swelling and inflammatory cell accumulation at 7 days (Figure 3D). Real-time imaging of inflammatory cell migration from the limbus towards the suture site 5 h after suture placement by *in vivo* confocal microscopy indicated significantly greater density and migration distance of granulocytes into Gap27-treated corneas relative to scGap27 (Figure 3E and F). After 2 and 7 days, inflammation was detectable at and beyond the suture site. Gene expression of IL-1β, TGFβ, IL-6 and TNF-α in the cornea did not differ between groups in the early phase of the wound healing process after 2 days (Figure 3G). However by day 7, TGFβ and TNFα were expressed at higher levels in Gap27-treated corneas (Figure 3H). The expression of Cx43 under both conditions did not differ after 2 or 7 days (Figure 3G and 3H), confirming that Gap27 blocks Cx43 without changing the expression of GJA1 or protein distribution of Cx43.

Effect of Gap27 on VEGFA expression and corneal neovascularization

Using the *ex vivo* human corneal SA model, the expression of VEGFA was detectable in all corneal layers. The positivity or pattern of VEGFA staining was not influenced by Gap27 treatment 6 h after injury. After 3 and 5 days, increased VEGFA expression towards the surface of the epithelial layer was observed in scGap27-treated corneas, while by day 7, both groups had similar expression profiles in the epithelium (Figure 4A). In terms of stromal expression, on day 1, VEGFA was detectable below the wound site in corneas treated with scGap27, while it was almost undetectable in the stroma of Gap27-treated corneas. Stromal positivity for VEGFA, however, had reversed by 7 days, when scGap27 corneas had almost absent staining, while staining in Gap27-treated corneas was apparent.

To determine VEGF release dynamics from human corneas after wounding, three pairs of corneas from three donors were incubated in the submerged culture system. A sharp decline in VEGFA release in scGap27 corneas was noted after 1 and 3 h ($P < 0.05$). In Gap27-treated corneas, however, VEGFA significantly decreased ($P < 0.05$) only after 3 h (Figure 4B).

In the *in vivo* rat corneal suture model, gene expression of VEGFA after 2 and 7 days from injury was not altered in Gap27-treated corneas as compared with corneas treated with scGap27 (Figure 4C). Additionally, there were no differences in the average limbal vessel dilation *in vivo* (Figure 4D). After 7 days, new invading blood vessels had reached past the sutured area (Figure 4G) in all corneas, and the vascularized area of the cornea did not differ between treatments (Figure 4E and F).

Discussion

Treatment with the Cx43 mimetic peptide Gap27 accelerated the rate of wound closure of human corneal epithelium *in vitro* and *ex vivo*. Formation of a fully differentiated layer of corneal epithelium was accelerated with Gap27 treatment; however, no suppression of inflammatory or angiogenic mediators was observed. Furthermore, treatment of rat corneas with Gap27 after deep stromal injury resulted in an increased rate of early granulocyte infiltration, late gene expression of TNF-α and TGFβ1 and there was no inhibitory effect on pathological neovascularization.

The beneficial wound healing properties evoked by blocking the gene expression of Cx43 are well documented (Kretz *et al.*, 2003; Brandner *et al.*, 2004; Cronin *et al.*, 2006; Nakano *et al.*, 2008; Bajpai *et al.*, 2009; Grupcheva *et al.*, 2012; Ormonde *et al.*, 2012). Cx43 knock-down accelerates the healing of corneal endothelial cells *in vivo* (Nakano *et al.*, 2008) and the re-epithelialization of persistent human corneal ulcers (Ormonde *et al.*, 2012). Additionally, blocking the protein function of Cx43 hemichannels using a specific peptide (α carboxy-terminus 1) was shown to be effective in accelerating the healing of corneal epithelial injuries in diabetic rats *in vivo* (Moore *et al.*, 2014). A recent clinical trial showed that the use of Cx43 mimetic peptides, α carboxy-terminus 1, enhanced the healing of persistent skin ulcers associated with chronic neuropathic diabetic patients (Grek *et al.*, 2015). With regard to Gap27, it has been shown to accelerate the wound healing of human organotypic skin model and human dermal fibroblasts *in vitro* (Pollok *et al.*, 2011; Wright *et al.*, 2012). In line with these findings, we observed that the treatment of human corneal epithelium with Gap27 accelerates cell migration and promotes wound closure rates.

Although this study and work by other groups has shown the potential of Gap27 as a wound healing agent, the underlying mechanisms of the effect of Gap27 on corneal wound healing requires an in-depth investigation. Hypotheses can be tested, for example, regarding the involvement of

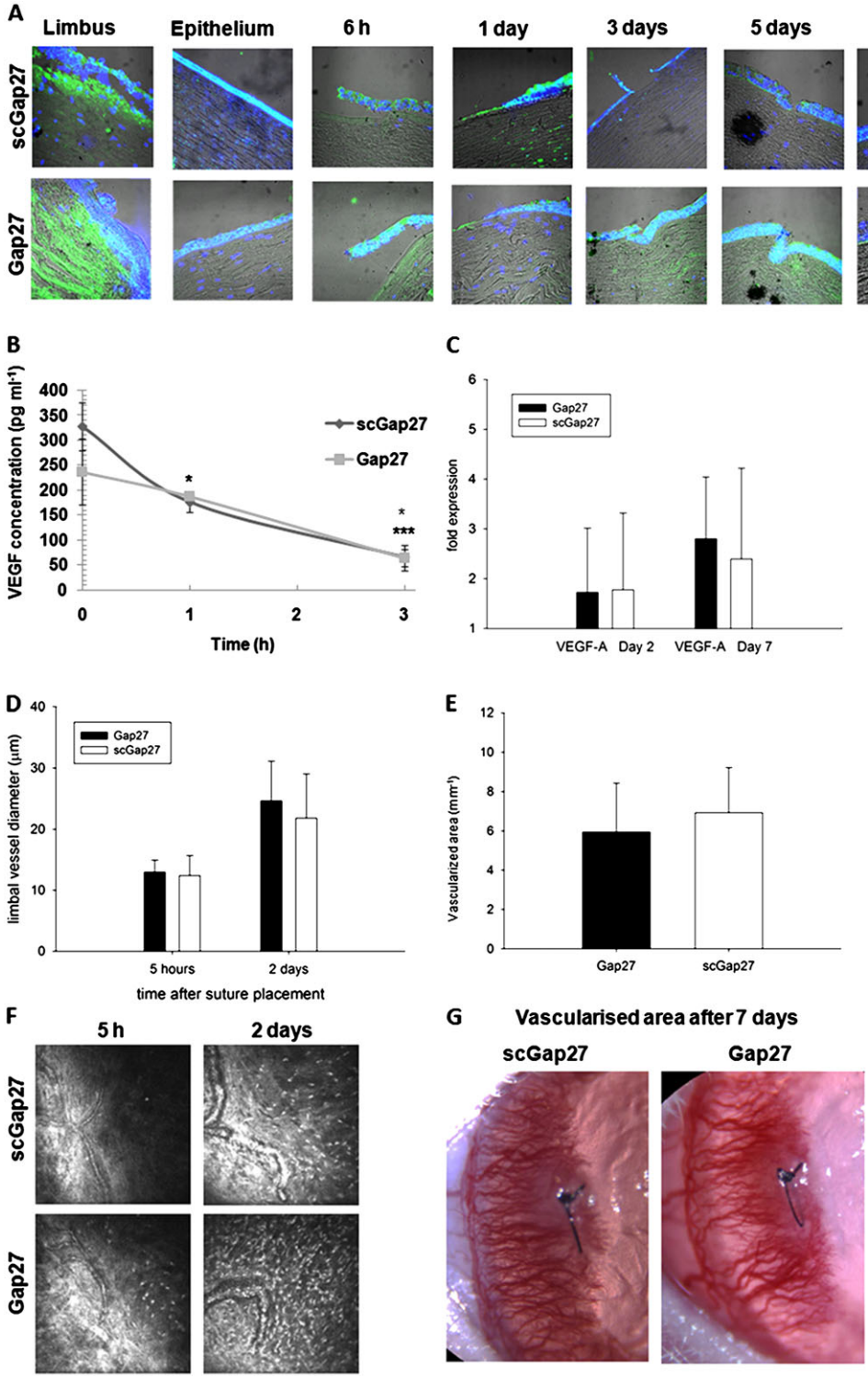

Figure 4

Gap27 treatment does not suppress VEGFA expression, vasodilatation or neovascularization. In the *ex vivo* model using the SA, VEGFA (green) was detected using specific antibodies labelled with FITC-conjugated secondary antibody (A). Nuclei were labelled with DAPI (blue). Images were taken using 40× lens of the laser scanning confocal microscope. Each image is representative of three images from three corneas. The concentration of VEGFA in media containing human corneas (submerged cultures) was detected using ELISA (B). Using the *in vivo* rat model, limbal vessels' diameters were measured using ImageJ software in three vessels in each of cornea and averaged (D). The total area of vascularization was measured (E) after 7 days of placing the suture in rat corneas. Each column in (D) and (E) represents an average from eight corneas ($n = 8$). Images taken by *in vivo* confocal microscopy (400 × 400 μm) are presented in (F) and slit lamp images of vascularized areas are represented in (G). * Indicates significant differences in Gap27-treated cultures compared with scGap27 where $P < 0.05$.

extracellular matrix (ECM) proteins in cell migration, which may be altered by Cx43 regulation. It was found that a Cx43 deficiency can induce the expression of ECM mediators (Zieske, 2001; Brandner *et al.*, 2008; Cogliati *et al.*, 2015). Blocking the gene expression of Cx43 using antisense oligonucleotides or blocking Cx43 channel function using specific peptides can alter collagen fibril organization, affecting cell motility (Lorraine *et al.*, 2015). However, non-channel functions of Cx43 such as ECM are proposed not to be directly affected by Gap27. Cx43 is also involved in gap junction-mediated intercellular communication. Using a dye transfer assay, gap junction communication was shown to be reduced by 40% in Cx43-deficient mice (Kretz *et al.*, 2003). Additionally, Gap27 was previously shown to reduce dye uptake in human keratinocytes (Pollok *et al.*, 2011). This can affect the exchange of inflammation and apoptosis signalling molecules, along with other molecules including ATP (Kang *et al.*, 2008). Not only is the channel function altered by Gap27, Ki67 positive cells were reported to increase after Gap27 treatment indicating an enhanced proliferation capacity (Pollok *et al.*, 2011), in line with previous findings (Mori *et al.*, 2006). Early wound closure appeared to be independent of limbal activity as the epithelium in the centre of the cornea migrates to close the gap (Huang and Tseng, 1991; Chang *et al.*, 2008). Hence, it is believed that the wound in the central corneal epithelium can heal independently from the limbal stem cells activity (Chang *et al.*, 2008). In line with these findings, we did not find any changes in the limbal stem cell marker P63 in scGap27- and Gap27-treated corneas (Supporting Information Figure S1). Finally, post-translational Cx43 phosphorylation has recently been proposed as a mechanism of action for Cx43 role in wound healing. Gap27 was shown to induce phosphorylation of Cx43 at Ser^{368}, reducing gap junction communication (Richards *et al.*, 2004; Solan and Lampe, 2014). These interesting data require further investigation to elucidate the relationship between cell migration and Cx43 blocking.

Cx43 is expressed by macrophages (Beyer and Steinberg, 1991), neutrophils (Jara *et al.*, 1995), lymphocytes (Oviedo-orta *et al.*, 2000) and mast cells (Vliagoftis *et al.*, 1999). The immune response secondary to tissue damage commences with an acute phase, when the neutrophils migrate to the wounded area and release inflammatory mediators affecting subsequent macrophage chemotaxis to the affected area. Cx43 mimetic peptides were reported to reduce inflammatory reactions to injury; however, the expression of TGFβ1 was not reduced after 1 day of treatment with siRNA against Cx43 in a rat model of endothelial injury (Nakano *et al.*, 2008), and a significant increase in TNF-α was detected in a diabetic rat model of epithelial injury after 3 days (Moore *et al.*, 2014). This increase was reversed after 5 days indicating that blocking Cx43 may promote an early inflammatory response. Our result of a delayed but significant increase in TGFβ1 and TNF-α expression *in vivo* provides further evidence for the promotion of inflammation. Similarly, a recent study confirmed that the expression to TGFβ1, alongside collagen types I and III and MMP2, increases after 7 days of inducing a skin wound in Cx43 heterozygous knockout mice as compared with controls (Cogliati *et al.*, 2015). A possible explanation may be due to the ability of Gap27 to penetrate to the stroma and promote early inflammatory cell migration, as noted in the early hours after corneal stromal wounding by a suture. After wound closure, the effect of Gap27 on the stroma is minimal, and therefore, the inflammation is not directly affected. However, contrary to our findings, inflammation was reported to be reduced in human corneas treated with ODN against Cx43 (Ormonde *et al.*, 2012). After Cx43 antisense ODN treatment, the number of neutrophils were reported to be 20% less around the lesion area after 1 and 2 days of inducing a wound in the skin of rats (Qiu *et al.*, 2003). Additionally, macrophage infiltration was reduced at days 2 and 7 post injury, while neutrophils were also detected in fewer quantities in days 1 and 2 in skin keratinocytes (Mori *et al.*, 2006). Down-regulation of Cx43 by ODN in the skin was shown to significantly reduce in fibroblasts the (C-C motif) ligand 2 after 2 days of injury and TNF-α by day 7, while no changes were observed after 1 day (Mori *et al.*, 2006). Our results suggest that in stromal wounds of the cornea, inflammation can be promoted by Cx43 inhibition-mediated cytokine expression and an associated accumulation of granulocytes and macrophages. The effects of Cx43 inhibition on cell migration and proliferation may therefore be limited not only to epithelial cells around the wound site where cytokine expression may be beneficial in a transient phase but also to inflammatory cells in the underlying stroma. A extended stromal inflammatory response in the avascular cornea may upset the immune balance leading to pathological neovascularization.

In the present study, an *in vivo* model was used as a better model to investigate inflammation and neovascularization because *in vitro* models are devoid of circulation-derived factors and effects. However, we attempted to minimize the use and the number of animals required to perform statistical analysis. In spite of the great deal of progress that has been made, there are currently few accepted non-animal alternative test methods for ocular irritancy. None of them uses human corneas. An *ex vivo* human cornea or whole eye can provide an essential contribution to the reduction of animal experiments in pharmaceutical and scientific research. The organ culture system we used is intended to reduce animal use in research (following the 3R principles). The advantages include the use of a human cornea, which is anatomically different from animal corneas, the sterile environment to prevent any interference with results, low-cost transferable technology and research-attractive features (Elbadawy *et al.*, 2015). This model is based on the well-established eye irritation tests and organ culture systems using living corneas obtained from animal eyes. The isolated rabbit, bovine or chicken eye test methods (Doucet *et al.*, 2006) are currently accepted by several regulatory agencies; however, a main negative aspect of such methods is the use of animal eyes, which differ anatomically from the human eye. For instance, an important protective layer of the cornea (Bowman's layer) is absent in rabbits (Cooper *et al.*, 2001; Cater and Harbell, 2006).

Corneal neovascularization is a threat to corneal transparency and visual acuity, which can ultimately result in compromising the vision significantly. Of note, tissue vascularization after injury can be helpful for certain tissues such as the skin or oral mucosal healing, but in the case of the cornea, it is desirable that wound healing agents suppress VEGF expression. The expression of VEGF in the cornea is a main indicator of possible neovascularization, and therefore, the

levels of VEGF are usually studied when testing new ocular medications of pharmacological agents. Using ODN to down-regulate Cx43 gene expression, re-epithelialization of the corneas with severe and persistent defects in five patients was achieved; however, vascularization of the corneas was evident after 1 year of treatment in two out of five patients (Ormonde *et al*., 2012). Regarding the expression of VEGF in human gingival fibroblasts treated with Gap27, an increased expression of VEGF was reported (Tarzemany *et al*. 2015). The accelerated re-epithelialization could be hypothesized to reduce corneal vascularization due to faster resolving of the initial wound since damaged epithelium can also be an important source of VEGF. However, our results suggested no beneficial effects of Gap27 on the suppression of VEGF or the subsequent vasodilation in limbal vessels, infiltration of granulocytes or vascularization after superficial or deep corneal injuries.

Overall, Gap27 could be effective in accelerating the healing of epithelial wounds in an early phase, but prolonged and frequent use in stromal wounds could elicit an undesirable inflammatory response. Accordingly, Gap27 use in the early stages of wound healing of the superficial corneal epithelial wounds can be proposed for promoting corneal epithelial healing in cases of persistent corneal ulcers, limbal stem cell deficiency and dry eye syndrome. However, Gap27 is not recommended for more invasive wounds involving the potential for stromal inflammation, such as with severe alkali burns, corneal transplantation and glaucoma filtration procedures.

Acknowledgements

The research leading to these results has received funding from the European Union Seventh Framework Program (FP7/2007-2013) under grant agreement no. 267232, Co-funding of Regional, National and International Programs 'Initiative for the Mobility and Development of researchers' careers (I-MOVE)'. The work is also supported by the European Cooperation in Science and Technology (EU-COST) program BM1302 'Joining Forces in Corneal Regeneration Research'; grant number COST-STSM-BM1302-24766. We also acknowledge the help of Dr. Nevine Bahaa, Dr. Mona Raafat and Prof. Amany ElShawarby from the Department of Histology, Faculty of Medicine, Ain Shams University in Cairo (Egypt) for their help with the interpretation of histological data.

Author contributions

H.M.E., C.C., D.P., N.L. and S.F. conceived and designed the experiments, H.M.E., M.X., P.M., M.B., C.B. and M.P., conducted the experiments. H.M.E., M.X., P.M., N.L. and S.F. performed the data analysis. H.M.E. wrote the manuscript which was revised by all authors.

Conflict of interest

The authors declare no conflicts of interest.

Declaration of transparency and scientific rigour

This Declaration acknowledges that this paper adheres to the principles for transparent reporting and scientific rigour of preclinical research recommended by funding agencies, publishers and other organisations engaged with supporting research.

References

Akar FG, Nass RD, Hahn S, Cingolani E, Shah M, Hesketh GG *et al.* (2007). Dynamic changes in conduction velocity and gap junction properties during development of pacing-induced heart failure. Am J Physiol Heart Circ Physiol 293: H1223–H1230.

Alexander SPH, Kelly E, Marrion N, Peters JA, Benson HE, Faccenda E *et al.* (2015a). The Concise Guide to PHARMACOLOGY 2015/16: Overview. Br J Pharmacol 172: 5729–5743.

Alexander SP, Kelly E, Marrion N, Peters JA, Benson HE, Faccenda E *et al.* (2015b). The concise guide to PHARMACOLOGY 2015/16: Other ion channels. Br J Pharmacol 172: 5942–5955.

Bajpai S, Shukla VK, Tripathi K, Srikrishna S, Singh RK (2009). Targeting connexin 43 in diabetic wound healing: Future perspectives. J Postgrad Med 5: 143–149.

Beyer E, Steinberg T (1991). Evidence that the gap junction protein connexin-43 is the ATP-induced pore of mouse macrophages. J Biol Chem 266: 7971–7974.

Brandner JM, Houdek P, Husing B, Kaiser C, Moll I (2004). Connexins 26, 30, and 43: differences among spontaneous, chronic, and accelerated human wound healing. J Investig Dermatol 122: 1310–1320.

Brandner JM, Zacheja S, Houdek P, Moll I, Lobmann R (2008). Expression of matrix metalloproteinases, cytokines, and connexins in diabetic and nondiabetic human keratinocytes before and after transplantation into an ex vivo wound-healing model. Diabetes Care 31: 114–120.

Castro-Munozledo F (2013). Review: corneal epithelial stem cells, their niche and wound healing. Mol Vis 19: 1600–1613.

Cater KC, Harbell JW (2006). Prediction of eye irritation potential of surfactant-based rinse-off personal care formulations by the bovine corneal opacity and permeability (BCOP) assay. Cutan Ocul Toxicol 25: 217–233.

Chang C-Y, Green CR, McGhee CNJ, Sherwin T (2008). Acute wound healing in the human central corneal epithelium appears to be independent of limbal stem cell influence. Invest Ophthalmol Vis Sci 49: 5279–5286.

Cogliati B, Vinken M, Silva TC, Araújo CM, Aloia TP, Chaible LM *et al.* (2015). Connexin 43 deficiency accelerates skin wound healing and extracellular matrix remodeling in mice. J Dermatol Sci 79: 50–56.

Cooper KJ, Earl LK, Harbell J, Raabe H (2001). Prediction of ocular irritancy of prototype shampoo formulations by the isolated rabbit eye (IRE) test and bovine corneal opacity and permeability (BCOP) assay. Toxicol In Vitro 15: 95–103.

Coutinho P, Qiu C, Frank S, Tamber K, Becker D (2003). Dynamic changes in connexin expression correlate with key events in the wound healing process. Cell Biol Int 27: 525–541.

Cronin M, Anderson PN, Green CR, Becker DL (2006). Antisense delivery and protein knockdown within the intact central nervous system. Front Biosci 11: 2967–2975.

Curtis MJ, Bond RA, Spina D, Ahluwalia A, Alexander S, Giembycz MA *et al.* (2015). Experimental design and analysis and their reporting: new guidance for publication in BJP. Br J Pharmacol 172: 3461–3471.

Di Iorio E, Ferrari S, Fasolo A, Böhm E, Ponzin D, Barbaro V (2010). Techniques for culture and assessment of limbal stem cell grafts. Ocul Surf 8: 146–153.

Doucet O, Lanvin M, Thillou C, Linossier C, Pupat C, Merlin B *et al.* (2006). Reconstituted human corneal epithelium: a new alternative to the Draize eye test for the assessment of the eye irritation potential of chemicals and cosmetic products. Toxicol In Vitro 20: 499–512.

Elbadawy HM, Salvalaio G, Parekh M, Ruzza A, Baruzzo M, Cagini C *et al.* (2015). A superfusion apparatus for ex vivo human eye irritation investigations. Toxicol In Vitro 29: 1619–1627.

Evans WH, Boitano S (2001). Connexin mimetic peptides: specific inhibitors of gap-junctional intercellular communication. Biochem Soc Trans 29: 606–612.

Goliger JA, Paul DL (1995). Wounding alters epidermal connexin expression and gap junction-mediated intercellular communication. Mol Biol Cell 6: 1491–1501.

Grek CL, Prasad G, Viswanathan V, Armstrong DG, Gourdie RG, Ghatnekar GS (2015). Topical administration of a connexin43-based peptide augments healing of chronic neuropathic diabetic foot ulcers: a multicenter, randomized trial. Wound Repair Regen 23: 203–212.

Grupcheva CN, Laux WT, Rupenthal ID, McGhee J, McGhee CNJ, Green CR (2012). Improved corneal wound healing through modulation of gap junction communication using connexin43-specific antisense oligodeoxynucleotides. Invest Ophthalmol Vis Sci 53: 1130–1138.

Huang A, Tseng S (1991). Corneal epithelial wound healing in the absence of limbal epithelium. Invest Ophthalmol Vis Sci 32: 96–105.

Jara PI, Boric MP, Saez JC (1995). Leukocytes express connexin 43 after activation with lipopolysaccharide and appear to form gap junctions with endothelial cells after ischemia–reperfusion. Proc Natl Acad Sci 92: 7011–7015.

Kang J, Kang N, Lovatt D, Torres A, Zhao Z, Lin J *et al.* (2008). Connexin 43 hemichannels are permeable to ATP. J Neurosci 28: 4702–4711.

Kilkenny C, Browne W, Cuthill IC, Emerson M, Altman DG (2010). NC3Rs Reporting Guidelines Working Group. Br J Pharmacol 160: 1577–1579.

Kretz M, Euwens C, Hombach S, Eckardt D, Teubner B, Traub O *et al.* (2003). Altered connexin expression and wound healing in the epidermis of connexin-deficient mice. J Cell Sci 116: 3443–3452.

Law LY, Zhang WV, Stott NS, Becker DL, Green CR (2006). In vitro optimization of antisense oligodeoxynucleotide design: an example using the connexin gene family. J Biomol Tech 17: 270.

Li Z, Zhou Z, Welch DR, Donahue HJ (2008). Expressing connexin 43 in breast cancer cells reduces their metastasis to lungs. Clin Exp Metastasis 25: 893–901.

Lorraine C, Wright CS, Martin PE (2015). Connexin43 plays diverse roles in co-ordinating cell migration and wound closure events. Biochem Soc Trans 43: 482–488.

Lu L, Reinach PS, Kao WWY (2001). Corneal epithelial wound healing. Exp Biol Med 226: 653–664.

Matic M, Petrov IN, Rosenfeld T, Wolosin JM (1997). Alterations in connexin expression and cell communication in healing corneal epithelium. Invest Ophthalmol Vis Sci 38: 600–609.

McGrath JC, Lilley E (2015). Implementing guidelines on reporting research using animals (ARRIVE etc.): new requirements for publication in BJP. Br J Pharmacol 172: 3189–3193.

McLachlan E, Shao Q, Wang H, Langlois S, Laird DW (2006). Connexins act as tumor suppressors in three-dimensional mammary cell organoids by regulating differentiation and angiogenesis. Cancer Res 66: 9886–9894.

Mirabelli P, Peebo BB, Xeroudaki M, Koulikovska M, Lagali N (2014). Early effects of dexamethasone and anti-VEGF therapy in an inflammatory corneal neovascularization model. Exp Eye Res 125: 118–127.

Moore K, Ghatnekar G, Gourdie RG, Potts JD (2014). Impact of the controlled release of a connexin 43 peptide on corneal wound closure in an STZ model of type I diabetes. PLoS One 9: e86570. doi:10.1371/journal.pone.0086570.

Mori R, Power KT, Wang CM, Martin P, Becker DL (2006). Acute downregulation of connexin43 at wound sites leads to a reduced inflammatory response, enhanced keratinocyte proliferation and wound fibroblast migration. J Cell Sci 119: 5193–5203.

Nakano Y, Oyamada M, Dai P, Nakagami T, Kinoshita S, Takamatsu T (2008). Connexin43 knockdown accelerates wound healing but inhibits mesenchymal transition after corneal endothelial injury *in vivo*. Invest Ophthalmol Vis Sci 49: 93–104.

Ormonde S, Chou C-Y, Goold L, Petsoglou C, Al-Taie R, Sherwin T *et al.* (2012). Regulation of connexin43 gap junction protein triggers vascular recovery and healing in human ocular persistent epithelial defect wounds. J Membr Biol 245: 381–388.

Oviedo-orta E, Hoy T, Evans WH (2000). Intercellular communication in the immune system: differential expression of connexin 40 and 43, and perturbation of gap junction channel functions in peripheral blood and tonsil human lymphocyte subpopulations. Immunology 99: 578–590.

Peebo BB, Fagerholm P, Traneus-Röckert C, Lagali N (2011). Cellular level characterization of capillary regression in inflammatory angiogenesis using an *in vivo* corneal model. Angiogenesis 14: 393–405.

Pollok S, Pfeiffer AC, Lobmann R, Wright CS, Moll I, Martin PEM *et al.* (2011). Connexin 43 mimetic peptide Gap27 reveals potential differences in the role of Cx43 in wound repair between diabetic and non diabetic cells. J Cell Mol Med 15: 861–873.

Qiu C, Coutinho P, Frank S, Franke S, Law L, Martin P *et al.* (2003). Targeting connexin43 expression accelerates the rate of wound repair. Curr Biol 13: 1697–1703.

Richards TS, Dunn CA, Carter WG, Usui ML, Olerud JE, Lampe PD (2004). Protein kinase C spatially and temporally regulates gap junctional communication during human wound repair via phosphorylation of connexin43 on serine368. J Cell Biol 167: 555–562.

Saitoh M, Oyamada M, Oyamada Y, Kaku T, Mori M (1997). Changes in the expression of gap junction proteins (connexins) in hamster tongue epithelium during wound healing and carcinogenesis. Carcinogenesis 18: 1319–1328.

Söhl G, Willecke K (2004). Gap junctions and the connexin protein family. Cardiovasc Res 62: 228–232.

Solan JL, Lampe PD (2014). Specific Cx43 phosphorylation events regulate gap junction turnover *in vivo*. FEBS Lett 588: 1423–1429.

Southan C, Sharman JL, Benson HE, Faccenda E, Pawson AJ, Alexander SP *et al.* (2016). The IUPHAR/BPS Guide to PHARMACOLOGY in 2016: towards curated quantitative interactions between 1300 protein targets and 6000 ligands. Nucleic Acids Res 44: D1054–D1068.

Tarzemany R, Jiang G, Larjava H, Häkkinen L (2015). Expression and function of connexin 43 in human gingival wound healing and fibroblasts. PLoS One 10.

Vliagoftis H, Hutson AM, Mahmudi-Azer S, Kim H, Rumsaeng V, Oh CK *et al.* (1999). Mast cells express connexins on their cytoplasmic membrane. J Allergy Clin Immunol 103: 656–662.

Wright CS, Van Steensel MA, Hodgins MB, Martin PE (2009). Connexin mimetic peptides improve cell migration rates of human epidermal keratinocytes and dermal fibroblasts in vitro. Wound Repair Regen 17: 240–249.

Wright CS, Pollok S, Flint DJ, Brandner JM, Martin PE (2012). The connexin mimetic peptide Gap27 increases human dermal fibroblast migration in hyperglycemic and hyperinsulinemic conditions in vitro. J Cell Physiol 227: 77–87.

Zieske JD (2001). Extracellular matrix and wound healing. Curr Opin Ophthalmol 12: 237–241.

Supporting Information

Additional Supporting Information may be found in the online version of this article at the publisher's web-site:

http://dx.doi.org/10.1111/bph.13568

Figure S1 Gap27 did not affect the expression pattern of Cx43, ZO-1, K12 or p63. In the ex vivo model using the SA, Cx43, ZO-1, K12 and p63 (all in green) were detected using specific antibodies labelled with FITC conjugated secondary antibody. Nuclei were labelled with DAPI nuclear staining (blue). Images were taken using 40x lens of the laser scanning confocal microscope. Each image is a representative of three images from three corneas at each time point.

Figure S2 Gap27 treatment did not induce apoptosis of cells in any corneal layer. Cell apoptosis analysis was done using TUNEL assay. Positive controls are corneas treated with hydrogen peroxide and negative controls are corneas treated with PBS. Images were taken using the 10x lens of a light microscope fitted with a digital camera.